Reliable Predictions of Benzophenone Singlet-Triplet Transition Rates: A Second-Order Cumulant Approach

Reliable Predictions of Singlet-Triplet Transition Rates: a Second Order Cumulant Approach

Amalia Velardo,*,† Alessandro Landi,‡ Raffaele Borrelli,¶ and Andrea Peluso‡

†*Department of Chemistry, University of Torino, Via P. Giuria, 7 - 10125 Torino, Italy, and Dipartimento di Chimica e Biologia Adolfo Zambelli, Università di Salerno, Via Giovanni Paolo II, I-84084 Fisciano (SA), Italy*

‡*Dipartimento di Chimica e Biologia Adolfo Zambelli, Università di Salerno, Via Giovanni Paolo II, I-84084 Fisciano (SA), Italy*

¶*Department of Agricultural, Forestry and Food Science, University of Torino, I-10195 Grugliasco, Italy*

E-mail: amalia.velardo@unito.it

Abstract

Fermi Golden Rule and second order cumulant expansion of the time dependent density matrix have been used to compute from first principles the rate of intersystem crossing in benzophenone, using minimum energy geometries and normal modes of vibrations computed at TDDFT/CAM-B3LYP level. Both approaches yield reliable values of the S_1 decay rate, the latter being almost in quantitative agreement with the results of time dependent spectroscopic measurements (0.154 ps^{-1} observed *vs.* 0.25 ps^{-1} predicted). Fermi Golden Rule slightly overestimates the decay rate of S_1 state (k_d=0.45 ps^{-1}), but provides better insights into the chemico-physical parameters which govern the transition from a thermally equilibrated population of S_1, showing that the indirect mechanism is much faster than the direct one because of the vanishingly small Franck-Condon weighted density of states at ΔE of transition.

Introduction

Singlet triplet transitions are of outstanding importance in photochemistry. Most of photochemical processes occur via triplet states because of their electronic activated character and comparatively longer lifetimes.[1] Triplet states also play a significant role in several processes of great technological importance: charge dissociation and charge recombination in photovoltaic solar cells,[2–7] electroluminesce in OLED,[8–11] and low power frequency upconversion.[12–15] It is therefore amenable to have efficient and reliable procedures for evaluating intersystem crossing (ISC) rates from quantities whose determination can be afforded by standard electronic computations, i.e. equilibrium geometries, normal modes of vibration, and spin orbit coupling elements. Herein we compare two alternative approaches for computing the rates of non radiative transitions between two electronic states: Fermi Golden Rule and second order cumulant average of the time dependent density matrix. Both approaches allow for considering thermal effects and for including in computations the whole set of normal coordinates, making use of closure relations for avoiding limitations on the number of quantum states to be considered in dynamics,[16–18] two fundamental points for obtaining reliable transition rates, which are difficult to meet in quantum dynamic simulations based on the numerical solution of the time dependent Schrödinger equation.

After a brief review concerning the implementation of both approaches with quantities obtained by first principle electronic calculations,[19–22] we will consider the fast ISC occurring in benzophenone as a test case for judging and comparing their performances, showing that the integrated use of the two approaches provides both an almost quantitative reproduction of the time dependent spectroscopic results of ISC in benzophenone and important chemico-physical insights for understanding mechanistic aspects of the process.

Methodology

Let us consider a system characterized by two electronic states $|i\rangle$ and $|f\rangle$ weakly coupled by a perturbation, whose Hamiltonian is given by:

$$\mathcal{H} = H_i \left|i\right\rangle \left\langle i\right| + H_f \left|f\right\rangle \left\langle f\right| + V_{if} \left|i\right\rangle \left\langle f\right| + cc = \mathcal{H}_0 + V, \tag{1}$$

where H_i and H_f are the vibrational Hamiltonians of the electronic states $|i\rangle$ and $|f\rangle$, and $V = V_{if} \left|i\right\rangle \left\langle f\right| + cc$. Both H_i and H_f are modeled in harmonic approximation:

$$H_i = \sum_i \frac{1}{2}\hbar\omega_i \left(\frac{d^2}{dq_i^2} + q_i^2\right)^2, \qquad H_f = \sum_f \frac{1}{2}\hbar\omega_f \left(\frac{d^2}{dq_f^2} + q_f^2\right)^2 \tag{2}$$

where $\omega_{i/f}$ and $q_{i/f}$ are the vibrational frequencies and the dimensionless normal coordinates of the state (i/f). The two sets of normal coordinates of $|i\rangle$ and $|f\rangle$ are related by Duschinki's transformation:

$$\mathbf{q}_f = \mathbf{J}\mathbf{q}_i + \mathbf{K}, \tag{3}$$

where $\mathbf{J}$ is the Duschinky's matrix, accounting for normal mode mixing, and $\mathbf{K}$ is the vector of equilibrium position displacements of $|f\rangle$ with respect to $|i\rangle$.

First order time dependent perturbation theory states that the transition rate from a distribution of initial states $ketim$ to a manifold of final states $|fn\rangle$ induced by a perturbation $\hat{V}$ is given by:

$$k_{i\to f} = \frac{2\pi}{\hbar} F(0, T) \tag{4}$$

with

$$F(E, T) = \sum_m \sum_n |\left\langle fn\right| \hat{V} \left|im\right\rangle|^2 w_m(T) \delta(E_{fn} - E_{im} - E) \tag{5}$$

where w_m is the probability of the m-th vibrational state of the electronic state $|i\rangle$. For a thermal equilibrium distribution $w_m = exp(-\beta E_{im})/Z_i$, with $\beta = 1/k_B T$ and $Z_i = \mathrm{Tr}\rho_i$, is the vibrational partition function of the initial state.

In the case the dependence of $\hat{V}$ upon the nuclear coordinates can be neglected, eq.n 5 can be rewritten as:

$$F(E,T) = |V_{if}|^2 \sum_m \sum_n |\langle fn|im\rangle|^2 w_m(T)\delta(E_{fn} - E_{im} - E) \tag{6}$$

where $|\langle fn|im\rangle|^2$ are the usual Franck-Condon factors.

The double summation over the whole set of vibrational states is avoided by evaluating the Laplace Transform of $F(E,T)$:

$$f(\lambda,T) = \int_{-\infty}^{\infty} F(E)exp(-\lambda E)dE = \sum_m \sum_n |\langle fn|\hat{V}|im\rangle|^2 e^{-\beta E_{im}} e^{-\lambda(E_{fn}-E_{im})}/\mathbf{Tr}\rho_i(\beta), \tag{7}$$

which can be recast into the form:

$$\begin{aligned} f(\lambda,T) &= \sum_m \sum_n \langle im|V|fn\rangle e^{-\lambda E_{fn}} \langle fn|\hat{V}|im\rangle e^{-(\beta-\lambda)E_{im}}/\mathbf{Tr}\rho_i(\beta) \\ &= \mathbf{Tr}V_{if}\rho_f(\lambda)V_{fi}\rho_i(\beta-\lambda)/\mathbf{Tr}\rho_i(\beta) \end{aligned} \tag{8}$$

where intractable summations are no longer present.

In the harmonic approximation the density matrix can be evaluated in closed form in the position representation:[17,23]

$$\begin{aligned} \rho_i(\mathbf{q}_i,\mathbf{q}'_i) = det\left[\frac{\Omega_i}{\sqrt{2\pi sinh(\beta\hbar\Omega_i)}}\right] \\ \times exp[-\frac{1}{4\hbar}(\mathbf{q}_i+\mathbf{q}'_i)^\dagger \Omega_i tanh(\beta\hbar\Omega_i/2)(\mathbf{q}_i+\mathbf{q}'_i) \\ -\frac{1}{4\hbar}(\mathbf{q}_i-\mathbf{q}'_i)^\dagger \Omega_i coth(\beta\hbar\Omega_i/2)(\mathbf{q}_i-\mathbf{q}'_i)] \end{aligned} \tag{9}$$

where $\mathbf{\Omega}_i$ is the diagonal matrix of harmonic vibrational frequencies of $|i\rangle$ a similar equation holding also for $\rho_f(\mathbf{q}_f,\mathbf{q}'_f)$. The trace in eqn. 8, which in the position representation corresponds to integration over the whole set of vibrational coordinates, can be analytically

carried out using Duschinsky's transformation of eqn. 3 and $f(\lambda)$ can be evaluated by standard multidimensional gaussian integration, see ref.s 20,21 for more details. Once $f(\lambda)$ is known, $F(E,T)$ can be obtained as the inverse Laplace transform of $f(\lambda)$, and transition rates computed by eqn. 4.

The Fermi Golden Rule (FGR) is based on the lowest order of time dependent perturbation theory and consider only direct transition. An alternative approach, which preserves most of the advantages of the previous treatment, relies on the second-order cumulant expansion of the time dependent density matrix of the system.[18,24–31]

For the Hamiltonian of eqn. 1, the time evolution of the density matrix in the interaction representation $\rho_I(t)$ is:

$$\rho_I(t) = \mathcal{T} \exp\left(-\frac{\mathrm{i}}{\hbar}\int_0^t V_I^{\times}(\tau)\mathrm{d}\tau\right)\rho_I(0) \tag{10}$$

where $\mathcal{T}$ is a time ordering operator and $V^{\times}$ is defined by $V_I^{\times}(\tau)\mathcal{O} = [V_I(\tau), \mathcal{O}]$.[26,32] $\rho_I(0)$ is the density matrix at time $t = 0$, specifying the initial conditions of the system. Formally, the population of the initial electronic state $|i\rangle$ is given by:

$$P_i(t) = \mathrm{Tr}\big\langle i\big|\mathcal{T} \exp\left(-\frac{\mathrm{i}\lambda}{\hbar}\int_0^t V_I^{\times}(\tau)\mathrm{d}\tau\right)\rho_I(0)\big|i\big\rangle \tag{11}$$

where the trace is taken over the unperturbed states and λ is a dummy variable which at the end of treatment is set to unity. In order to introduce the cumulant expansion we make the ansatz:[24]

$$P_i(t) = e^{K(t)} \tag{12}$$

and expand $K(t)$ in a Taylor series of the dummy variable λ:

$$K(t) = \lambda k_1(t) + \lambda^2 k_2(t) + ... \tag{13}$$

By expanding perturbatively eq.n 11 and comparing with the expansion of $K(t)$ truncated

at the second order,[24,33] the first two cumulants are:

$$\begin{aligned} k_1(t) &= -\frac{i}{\hbar}\int_0^t \mathrm{d}\tau_1 V_I^{\times}(\tau_1)\rho_I(0) \\ k_2(t) &= -\frac{1}{2\hbar^2}\int_0^t \mathrm{d}\tau_1 \int_0^t \langle i|\left[V_I(\tau_1),\left[V_I(\tau_2),\rho(0)\right]\right]|i\rangle \,\mathrm{d}\tau_2. \end{aligned} \tag{14}$$

It is important to notice that with the Hamiltonian of eq.n 1 all odd-order cumulant terms are zero, because of orthogonality of the electronic wavefunctions and the first non null contributions are given by the second-order terms of cumulant expansion. To better understand the physical meaning of cumulant expansion, we differentiate eqn. 12, obtaining the rate of change of $|i\rangle$ population:

$$W_i = k(t)P_i(t), \tag{15}$$

where $k(t)$ is a time dependent rate constant for the $i \to f$ transition.

In the case the initial density coincides with the thermal distribution of the initial state $|i\rangle$ ($\rho(0) = \frac{1}{Z_i}|i\rangle e^{-\beta H_i}\langle i|$) and the coupling operator is independent of coordinate (a very reasonable assumption in the case the transition occurs by tunneling because of the small region spanned by the vibrational coordinates of the initial state), $k(t)$, after integration over the electronic coordinates, takes the form:

$$\begin{aligned} k(t) &= -\frac{1}{\hbar^2 Z_i}|V_{if}|^2\int_0^t d\tau f(\tau), \\ f(\tau) = \mathrm{Tr} e^{iH_i(\tau+i\beta)/\hbar}e^{-iH_f(\tau)/\hbar} &= \int d\mathbf{q_i}\,\langle \mathbf{q_i}|\, e^{iH_i(\tau+i\beta)/\hbar}e^{-iH_f(\tau)/\hbar}\,|\mathbf{q_i}\rangle \\ &= \int d\mathbf{q_i}d\mathbf{q_i'}\rho_i(\mathbf{q_i},\mathbf{q_i'},\beta-i\tau)\rho_f(\mathbf{q_f},\mathbf{q_f'},i\tau) \end{aligned} \tag{16}$$

Using eqn.s 9 and 3 $f(\tau)$ can be evaluated by standard multidimensional gaussian integration,[34] and $k(t)$ by numerical integration.

Noteworthy, cumulant second order expansion allows also the use of non equilibrium population of the initial state. That is an important point in treating ultrafast transitions

upon photo-excitation by a short time laser pulse.[35] In that case, the resulting initial density is just the Boltzmann equilibrium distribution of the ground state (GS) projected onto the photoexcited state $|i\rangle$:

$$\rho(0) = \frac{1}{Z_{GS}} |i\rangle \, e^{-\beta H_{GS}} \, \langle i| \tag{17}$$

and $k(t)$ assumes the form:

$$k(t) = -\frac{1}{\hbar^2 Z_G S} |V_{if}|^2 \int_0^t d\tau \mathrm{Tr} e^{-\beta H_{GS}} e^{itH_i/\hbar} e^{-i\tau H_f/\hbar} e^{-i(t-\tau)H_i/\hbar} \tag{18}$$

Furthermore, the second order cumulant approach can be applied to any coupling operator having the form of a power series expansion either in the vibrational coordinates or momenta. It is thus of interest for the analysis of the dynamics of electron-transfer reactions as well as of ultrafast radiationless transitions induced by conical intersections.

Intersystem crossing in benzophenone

Benzophenone is a paradigmatic example of fast singlet triplet transition, exhibiting almost unit quantum efficiency with a consequent absence of fluorescence emission under the usual excitation conditions.[36] Recent time-resolved absorption spectroscopy has revealed that ISC in benzophenone occurs on timescales of 10-20 ps, indipendently of the solvent.[37] Decomposition of the time-resolved spectra into pure spectra of transient species and their associated time-dependent concentrations suggested the possible implication in the S_1 relaxation process of electronic states other than T_1.

The possibility that ISC in benzophenone could not be an elementary process was already arised,[36,38] both because S_1 and T_1 are believed to share the same electronic character, so that, according to El Sayed rule, the spin orbit coupling (SOC) between them is expected to be vanishingly small, and because sensitized phosphorescence spectra of jet-cooled benzophenone had shown that $T_1 \leftarrow S_0$ transition is very similar in its vibrational structure to

the $S_1 \leftarrow S_0$ one. This observation indicates that the two electronic states possess an almost identical geometrical structure, resulting into a vanishingly small Franck-Condon factor for the direct $S_1 \rightarrow T_1$ transition, apart from a restricted energy region around $\Delta E = 0$.[38] It was therefore argued that the $S_1 \rightarrow T_1$ transition could take place along an indirect pathway $S_1 \rightarrow T_n \rightarrow T_1$, where T_n is a (π,π^*) excited triplet states, lying slightly higher in energy than T_1. Evidence about the possible existence of such T_n state was provided by time-resolved infrared absorption spectrum of photoexcited benzophenone, which exhibits a broad electronic absorption band in the wavenumber region above 2000 cm^{-1}.[39] Similar conclusions about the possibility of an indirect mechanism for the $S_1 \rightarrow T_1$ transition were also reached by following the decay dynamics of excited benzophenone by time resolved photoelectron spectroscopy.[40]

The difficulty concerning the small SOC element is not very stringent: benzophenone is not planar, neither in the ground state nor in the low lying excited states, and that could mix to some extent (n,π^*) and (π,π^*) states,[41] providing SOC high enough for the direct mechanism.[41–43] The second difficulty with the direct mechanism, i.e. the small Franck-Condon factor for the direct transition, has not been addressed in the literature yet, and we start our analysis of fast ISC in benzophenone by computing the Franck-Condon weighted density of states (FCWDS) for both the $S_1 \rightarrow T_1$ transition and $S_1 \rightarrow T_2$ transition. Computations have been performed by using the generating function approach outlined in the previous section, which provided very reliable spectroscopic band shapes both for benzophenone and for difficult cases as cyanines.[44–46] Optimized geometries and normal modes have been obtained at TDDFT/CAM-B3LYP/TZVP level of computations. The computed FCWDS for the $S_1 \rightarrow T_1$ and $S_1 \rightarrow T_2$ transitions as a function of the energy difference between initial and final states are reported in figure 1 and 2. Inspection of figure 1 shows that the FCWDS for the direct S1 $\rightarrow T_1$ transition at T=298 K is a very narrow function of ΔE, the energy difference between the two states, peaked at $\Delta E \approx 0$. For ΔE as small as 500 cm^{-1}, the FCWDS is already vanishingly small, as it would be expected from the observed band shapes

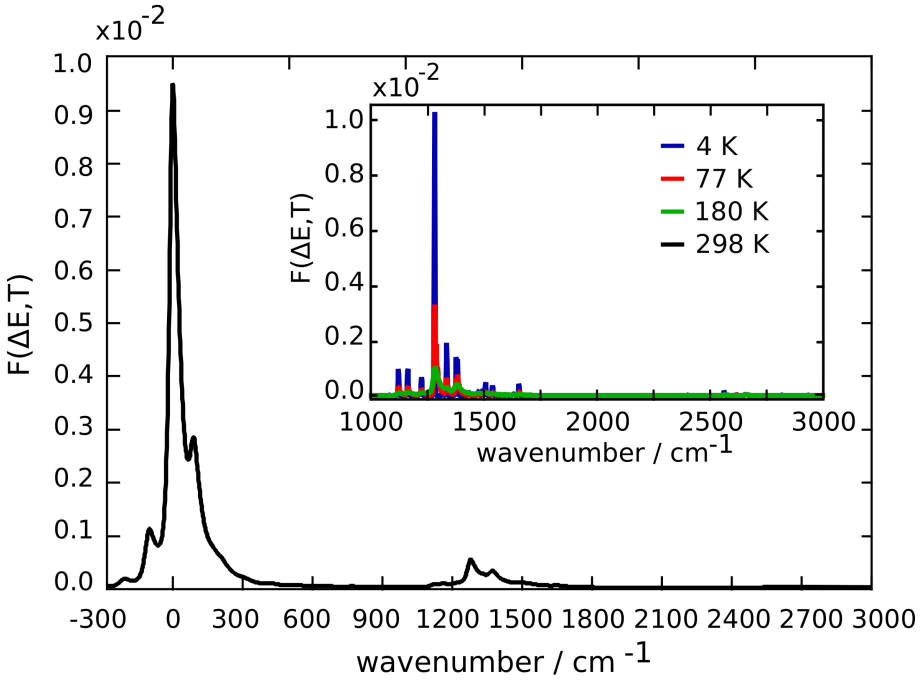

Figure 1: The Franck-Condon weighted density of states for the $S_1 \rightarrow T_1$ transition at T=298 K and, inset, at T= 4, 77, 180 K.

of $T_1 \leftarrow S_0$ and $S_1 \leftarrow S_0$ radiative transitions.[38] The FCWDS slightly rises into a short ΔE region between 1200-1500 cm^{-1}, because of displaced vibrational coordinates falling in that frequency region, roughly corresponding to the bending and asymmetric stretching involving the carbonyl group and adjacent ring carbons and the stretching of the C=O bond. ΔE for the $S_1 \rightarrow T_1$ transition can be obtained from the assignments of the 0-0 transitions of the $S_1 \leftarrow S_0$ absorption spectrum and the $T_1 \rightarrow S_0$ phosphorescence spectrum, falling at 26244 cm^{-1},[47] and 23800 cm^{-1},[48] respectively. Using such ΔE (2444 cm^{-1}) and the computed SOC (28.58 cm^{-1}, our own computation at S_1 minimum energy geometry) the resulting rate constant for the elementary transition is $\approx 1 \times 10^8 s^{-1}$, with a decay time of the order of nanoseconds, much longer than that found from time resolved spectroscopic measurements.[36,37,40] This situation does not modify by changing the temperature, as shown by the inset of figure 1 where the results obtained at different T are reported.

By contrast, $F(\Delta E, T)$ for the $S_1 \rightarrow T_2$ transition is a broad function of ΔE, extending from -500 to 20000 cm^{-1}, as shown in figure 2. Time-resolved infrared absorption spectra

of photoexcited benzophenone in carbon tetrachloride and benzene have shown a broad electronic absorption band ascribable to the $T_2 \leftarrow T_1$ transition in the wavenumber region above 2000 cm^{-1},[39] so that T_2 is expected to be almost isoenergetic with S_1, in good agrement with CAM-B3LYP/TDDFT computations, which predict an electronic energy difference of ≈400 cm^{-1}. The average value of $F(\Delta E, T)$ for the $S_1 \rightarrow T_2$ transition, taken over a range of ±300 cm^{-1}around $\Delta E = 400$ cm^{-1}, is $\approx 1 \times 10^{-4}$, the computed SOC element is 31.00 cm^{-1}(our own computation at S_1 minimum energy geometry), and the resulting FGR rate constant for the $S_1 \rightarrow T_2$ transition is 4.54×10^{11}. Thus FGR predicts that the indirect decay mechanism is significantly faster than direct one, in line with what would be suggested by the analysis of time resolved spectral signals, yielding a S_1 decay rate slightly faster than the observed one. The second-order cumulant expansion of the time dependent density matrix should provide an improvement with respect to FGR, inasmuch as it allows to obtain time dependent populations rather than time independent transition rates.

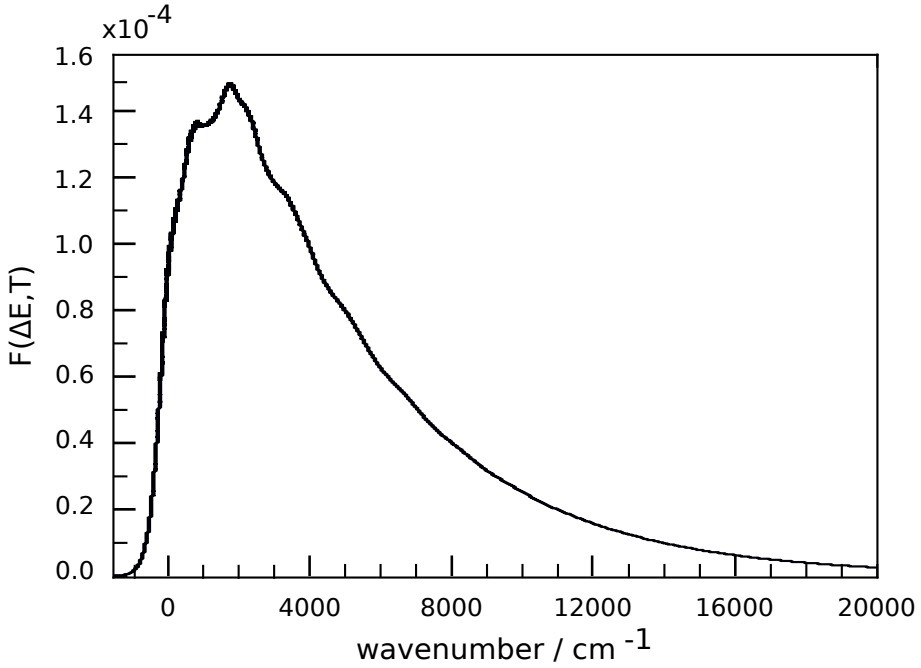

Figure 2: Franck-Condon weighted densities of states for $S_1 \rightarrow T_2$ transition as a function of the energy difference between the electronic states ($\Delta E = E_{S_1} - E_{T_2}$) at T = 298K.

The results obtained by second order cumulant expansion are shown in figure 3, both

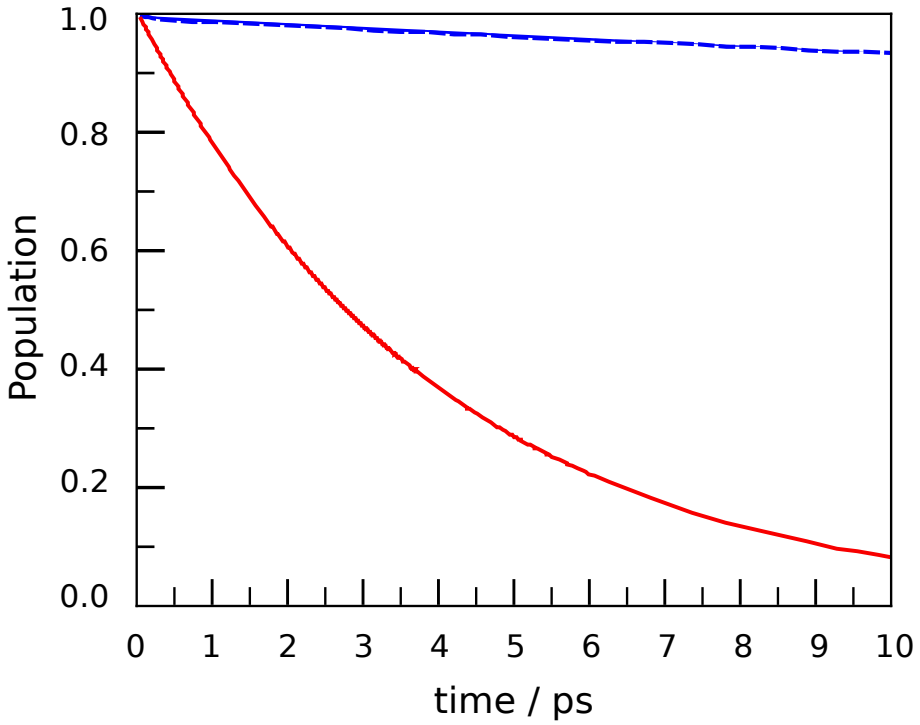

Figure 3: Decay rates of S_1 state of benzophenone predicted by second order cumulant expansion of the time dependent density matrix Franck-Condon weighted densities of states for both $S_1 \rightarrow T_2$ (red full lines) and $S_1 \rightarrow T_1$ (blue dashed lines) transitions.

for the $S_1 \rightarrow T_2$ and $S_1 \rightarrow T_1$ transitions. In line with FGR results, second order cumulant expansion predicts that the $S_1 \rightarrow T_1$ is much slower than $S_1 \rightarrow T_2$ one. For the latter transition, the average S_1 decay rate is $k_d = 0.25$ ps^{-1}, in very good agreement with experimental result of Aloïsi et al, (k_d=0.25 ps^{-1}), the average rate for the direct mechanism is ca. two order of magnitude slower (k_d=6 ns^{-1}). The above results an equilibrium initial distribution of ρ_0:

$$\rho_i(0) = Z_{S_1} |S_1\rangle e^{-\beta \mathcal{H}_{S1}} \langle S_1| \tag{19}$$

The second order cumulant expansion allows also a physically meaningful use of a non equilibrium distribution of the initial state, as necessary for ultrafast processes in which the initial state is prepared by a short laser pulse. In that case the initial distribution of states can be modeled by the thermally equilibrated distribution of the ground state, c.f. eqn. 17, and $k(t)$ is given by eqn. 18. S_1 decay of benzophenone is not an ultrafast process,

the population of the initial state has likely time enough to relax to a thermal distribution, before the transition occurs. Evidence in that direction comes from the fact that S_1 decay time is almost independent of the excitation wavelength, the observed S_1 decay rates being 0.154 ps^{-1} for excitation in S_2 at 267 nm and 0.133 ps^{-1} for excitation at 383 nm, which is just sufficient to populate the lowest energy vibrational states of S_1. Notwithstanding, just for speculative purposes, we have also considered the dynamics of S_1 decay for a non equilibrium population, originated by a very short laser pulse, projecting the ground state equilibrium populations of S_0 on S_1. The results are reported in figure 4. Inspection of figure 4 shows that a non equilibrium population of S_1 activates the direct transition, even though the indirect one remains slightly faster and therefore well competitive with the direct one. The effect is significant because it increases the rate of the direct one by ca. two order of magnitude, the time average rate for the $S_1 \rightarrow T_1$ being ca. 0.16 ps^{-1}. The different choice of the initial state has little importance for the $S_1 \rightarrow T_2$ transition: the predicted average decay rate changes from 0.25 ps^{-1} to 0.22 ps^{-1} for the initial equilibrium and non-equilibrium distribution, respectively.

In conclusion, our analysis clearly shows that the indirect mechanism is more plausible than direct one, because of the small Franck-Condon weighted density of states associated with the direct transition, as it was already argued from the analysis of the absorption and sensitized phosphorescence spectra of jet-cooled benzophenone. Both FGR and the second order cumulant expansion of the time dependent density matrix provide a faithful (at least as concerns comparison with time dependent spectroscopic measurements) description of the dynamics of intersystem crossing in benzophenone, which, at least for benzophenone, appears to be more reliable than those obtained by QM/MM approach.[42,43] The full quantum mechanical approaches proposed here cannot handle cases in which the equilibrium geometries of the two electronic states are significantly displaced each other – the case for instance of conformationally gated transitions – and all those cases in which environment fluctuations provide the driving force for electronic transitions, as for electron transfer reactions in polar

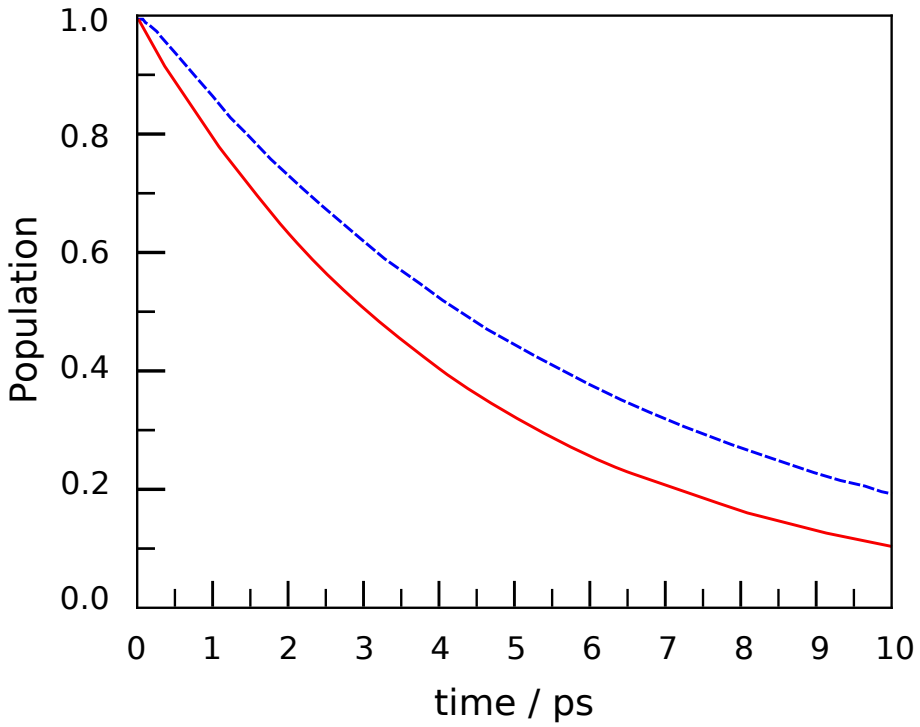

Figure 4: Decay rates of S_1 state of a non equilibrium initial distribution of benzophenone predicted by second order cumulant expansion of the time dependent density matrix for both $S_1 \rightarrow T_2$ (red full lines) and $S_1 \rightarrow T_1$ (blue dashed lines) transitions.

solvents.[49–51] In those cases, as also argued elsewhere,[51] the present approach could however be integrated into QM/MM simulation, the latter providing either the reactive conformations as stable minimum points of the electronic energy hypersufaces or the frequencies of solvent fluctuations.

Computational details

Computations of the equilibrium positions and vibrational frequencies of S_1, T_1, and T_2 states for benzophenone in the gas phase have been carried out at the density functional level of theory (DFT), with CAM-B3LYP functional and TZVP basis set, using the Gaussian package;[52] for triplet states the unrestricted formalism has been used and time dependent DFT (TDDFT) was used for excited states. All electronic states have been fully optimized; the computed vibrational frequencies are all positive, ensuring about the localization of

genuine minimum equilibrium structures.

SOC matrix elements have been computed by PySOC code,[53] at the equilibrium geometry of S_1; the SOC elements are 28.58 and 31.00 cm^{-1} for $S_1 \rightarrow T_1$ and $S_1 \rightarrow T_2$ transitions, respectively.

The Duschinsky matrix **J** and the displacement vector **K**, necessary to carry out the trace operation of eq. 8, have been computed using the curvilinear coordinate representation of the normal modes as implemented in a locally modified version of the MolFC software.[54,55] The use of internal coordinates prevents unphysical large shifts of the involved bond distances caused by large displacements of angular coordinates.[56–60] FGR rate constants have been computed by using an average value of $F(\Delta E, T)$, taken over a range of ± 0.05 eV around the corresponding ΔE values.

References

(1) Turro, N. J. *Modern Molecular Photochemistry*; University Science Books, 1991.

(2) Veldman, D.; Meskers, S. C. J.; Janssen, R. A. J. The Energy of Charge-Transfer States in Electron Donor-Acceptor Blends: Insight into the Energy Losses in Organic Solar Cells. *Adv. Funct. Mater.* **2009**, *19*, 1939–1948.

(3) Piliego, C.; Loi, M. A. Charge Transfer State in Highly Efficient Polymer-Fullerene Bulk Heterojunction Solar Cells. *J. Mater. Chem.* **2012**, *22*, 4141–4150.

(4) Rao, A.; Chow, P. C. Y.; Gélinas, S.; Schlenker, C. W.; Li, C.-Z.; Yip, H.-L.; Jen, A. K.-Y.; Ginger, D. S.; Friend, R. H. The Role of Spin in the Kinetic Control of Recombination in Organic Photovoltaics. *Nature* **2013**, *500*, 435–439.

(5) Chow, P. C. Y.; Albert-Seifried, S.; Gélinas, S.; Friend, R. H. Nanosecond Intersystem Crossing Times in Fullerene Acceptors: Implications for Organic Photovoltaic Diodes. *Adv. Mater.* **2014**, *26*, 4851–4854.

(6) Gélinas, S.; Rao, A.; Kumar, A.; Smith, S. L.; Chin, A. W.; Clark, J.; van der Poll, T. S.; Bazan, G. C.; Friend, R. H. Ultrafast Long-Range Charge Separation in Organic Semiconductor Photovoltaic Diodes. *Science* **2014**, *343*, 512–516.

(7) Velardo, A.; Borrelli, R.; Capobianco, A.; La Rocca, M. V.; Peluso, A. First Principle Analysis of Charge Dissociation and Charge Recombination Processes in Organic Solar Cells. *J. Phys. Chem. C* **2015**, *119*, 18870–18876.

(8) Uoyama, H.; Goushi, K.; Shizu, K.; Nomura, H. ; Adachi, C. Highly Efficient Organic Light-Emitting Diodes From Delayed Fluorescence. *Nature* **2012**, *492*, 234–238.

(9) Park, I.; Matsuo, K.; Aizawa, N. High-Performance Dibenzoheteraborin-Based Thermally Activated Delayed Fluorescence Emitters: Molecular Architectonics for Concurrently Achieving Narrowband Emission and Efficient Triplet-Singlet Spin Conversion. *Adv. Func. Mat.* **2018**, *06*, 1802031.

(10) Baldo, M.; O'Brien, D.; You, Y.; Shoustikov, A.; Sibley, S.; Thompson, M. E.; Forrest, S. R. Highly Efficient Phosphorescent Emission from Organic Electroluminescent Devices. *Nature* **1998**, *395*, 151–154.

(11) Baldo, M. A.; Thompson, M. E.; Forrest, S. R. High-Efficiency Fluorescent Organic Light-Emitting Devices Using a Phosphorescent Sensitizer. *Nature* **2000**, *403*, 750–753.

(12) Baluschev, S.; Miteva, T.; Yakutkin, V.; Nelles, G.; Yasuda, A.; Wegner, G. Up-Conversion Fluorescence: Noncoherent Excitation by Sunlight. *Phys. Rev. Lett.* **2006**, *97*, 143903.

(13) Ye, C.; Wang, X., J.and Wang; Ding, P.; Liang, Z.; Tao, X. A New Medium for Triplet-Triplet Annihilated Upconversion and Photocatalytic Application. *Phys. Chem. Chem. Phys.* **2016**, *18*, 3430–3437.

(14) Khnayzer, R. S.; Blumhoff, J.; Harrington, J. A.; Haefele, A.; Deng, F.; Castellano, F. N. Upconversion-powered Photoelectrochemistry. *Chem. Commun.* **2012**, *48*, 209–211.

(15) Della Sala, P.; Capobianco, A.; Caruso, T.; Talotta, C.; De Rosa, M.; Neri, P.; Peluso, A.; Gaeta, C. An Anthracene-Incorporated [8]Cycloparaphenylene Derivative as an Emitter in Photon Upconversion. *J. Org. Chem.* **2018**, *83*, 220–227.

(16) Lax, M. The Franck-Condon Principle and Its Application to Crystals. *J. Chem. Phys.* **1952**, *20*, 1752–1760.

(17) Kubo, R.; Toyozawa, Y. Application of the Method of Generating Function to Radiative and Non-Radiative Transitions of a Trapped Electron in a Crystal. *Prog. Theor. Phys.* **1955**, *13*, 160–182.

(18) Kubo, R. Generalized Cumulant Expansion Method. *J. Phys. Soc. Jap.* **1962**, *17*, 1100–1120.

(19) Peng, Q.; Yi, Y.; Shuai, Z.; Shao, J. Excited state radiationless decay process with Duschinsky rotation effect: Formalism and implementation. *J. Chem. Phys.* **2007**, *126*, 114302.

(20) Raffaele, B.; Andrea, P. The Temperature Dependence of Radiationless Transition Rates from Ab Initio Computations. *Phys. Chem. Chem. Phys.* **2011**, *13*, 4420–4426.

(21) Etinski, M.; Tatchen, J.; Marian, C. M. Time-dependent Approaches for the Calculation of Intersystem Crossing Rates. *J. Chem. Phys.* **2011**, *134*, 154105.

(22) Borrelli, R.; Capobianco, A.; Peluso, A. Generating Function Approach to the Calculation of Spectral Band Shapes of Free-Base Chlorin Including Duschinsky and Herzberg-Teller Effects. *J. Phys. Chem. A* **2012**, *116*, 9934–9940.

(23) Feynman, R. P. *Statistical Mechanics: A Set of Lectures*; Taylor & Francis Group, 1972.

(24) Mukamel, S. *Principles of Nonlinear Optical Spectroscopy*; OXFORD UNIVERSITY PRESS, 1995; Chapter 3.

(25) Breuer, H.-P.; Ma, A.; Petruccione, F. Time-local Master Equations: Influence Functional and Cumulant Expansion. 2002.

(26) Kubo, R. Stochastic Liouville Equations. *J. Math. Phys.* **1963**, *4*, 174–183.

(27) Van Kampen, N. A Cumulant Expansion for Stochastic Linear Differential equations. I. *Physica* **1974**, *74*, 215 – 238.

(28) Nitzan, A.; Jortner, J. Vibrational Relaxation of a Molecule in a Dense Medium. *Mol. Phys.* **1973**, *25*, 713–734.

(29) Izmaylov, A. F.; Mendive-Tapia, D.; Bearpark, M. J.; Robb, M. A.; Tully, J. C.; Frisch, M. J. Nonequilibrium Fermi Golden Rule for Electronic Transitions Through Conical Intersections. *J. Chem. Phys.* **2011**, *135*, 234106.

(30) Pereverzev, A.; Bittner, E. R. Time-Convolutionless Master Equation for Mesoscopic Electron-Phonon Systems. *J. Chem. Phys.* **2006**, *125*, 104906.

(31) Jang, S.; Cao, J.; Silbey, R. J. Fourth-order Quantum Master Equation and its Markovian Bath Limit. *J. Chem. Phys.* **2002**, *116*, 2705–2717.

(32) Fox, R. F. Critique of the Generalized Cumulant Expansion Method. *J. Math. Phys.* **1976**, *17*, 1148–1153.

(33) Magnus, W. On the Exponential Solution of Differential Equations for a Linear Operator. *Commun. Pure Appl. Matematica* **1954**, *7*, 649–673.

(34) Borrelli, R.; Capobianco, A.; Landi, A.; Peluso, A. Vibronic Couplings and Coherent Electron Transfer in Bridged Systems. *Phys. Chem. Chem. Phys.* **2015**, *17*, 30937–30945.

(35) Parson, W. W.; Warshel, A. Dependence of Photosynthetic Electron-Transfer Kinetics on Temperature and Energy in a Density-Matrix Model. *J. Phys. Chem. B* **2004**, *108*, 10474–10483.

(36) RENTZEPIS, P. M. Ultrafast Processes. *Science* **1970** *169*, 239–247.

(37) Aloïse, S.; Ruckebusch, C.; Blanchet, L.; Réhault, J.; Buntinx, G.; Huvenne, J.-P. The Benzophenone S1(n,π^*) $\rightarrow$ T1(n,π^*) States Intersystem Crossing Reinvestigated by Ultrafast Absorption Spectroscopy and Multivariate Curve Resolution. *J. Phys. Chem. A* **2008**, *112*, 224–231.

(38) Ohmori, N.; Suzuki, T.; Ito, M. Why Does Intersystem Crossing Occur in Isolated Molecules of Benzaldehyde, Acetophenone, and Benzophenone? *J. Phys. Chem.* **1988**, *92*, 1086–1093.

(39) Yabumoto, S.; Sato, S.; o Hamaguchi, H. Vibrational and Electronic Infrared Absorption Spectra of Benzophenone in the Lowest Excited Triplet State. *Chem. Phys. Lett.* **2005**, *416*, 100–103.

(40) Spighi, G.; Gaveau, M.-A.; Mestdagh, J.-M.; Poisson, L.; Soep, B. Gas Phase Dynamics of Triplet Formation in Benzophenone. *Phys. Chem. Chem. Phys.* **2014**, *16*, 9610–9618.

(41) Sergentu, D.-C.; Maurice, R.; Havenith, R. W. A.; Broer, R.; Roca-SanjuÃąn, D. Computational Determination of the Dominant Triplet Population Mechanism in Photoexcited Benzophenone. *Phys. Chem. Chem. Phys.* **2014**, *16*, 25393–25403.

(42) Marazzi, M.; Mai, S.; Roca-Sanjuán, D.; Delcey, M. G.; Lindh, R.; González, L.; Monari, A. Benzophenone Ultrafast Triplet Population: Revisiting the Kinetic Model by Surface-Hopping Dynamics. *J. Phys. Chem. Lett.* **2016**, *7*, 622–626.

(43) Favero, L.; Granucci, G.; Persico, M. Surface Hopping Investigation of Benzophenone Excited State Dynamics. *Phys. Chem. Chem. Phys.* **2016**, *18*, 10499–10506.

(44) Capobianco, A.; Borrelli, R.; Landi, A.; Velardo, A.; Peluso, A. Absorption Band Shapes of a Push-Pull Dye Approaching the Cyanine Limit: A Challenging Case for First Principle Calculations. *J. Phys. Chem. A* **2016**, *120*, 5581–5589.

(45) Velardo, A.; Borrelli, R.; Peluso, A.; Capobianco, A. First-Principle Calculations of the Band Shapes of Singlet-Triplet Transitions. *J. Phys. Chem. C* **2016**, *120*, 24605–24614.

(46) Velardo, A.; Borrelli, R.; Capobianco, A.; Landi, A.; Peluso, A. Disentangling Electronic and Vibrational Effects in the Prediction of Band Shapes for Singlet-Triplet Transitions. *J. Phys. Chem. C* **2019**, *123*, 14173–14179.

(47) Kamei, S.; Sato, T.; Mikami, N.; Ito, M. $n, \pi*$ State of Jet-Cooled Benzophenone as Studied by Sensitized Phosphorescence Excitation Spectroscopy. *J. Phys. Chem.* **1986**, *90*, 5615–5619.

(48) McClure, D. S.; Hanst, P. L. Excited Triplet States of Polyatomic Molecules. II. Flash-Lamp Studies on Aromatic Ketones. *J. Chem. Phys.* **1955**, *23*, 1772–1777.

(49) Landi, A.; Troisi, A.; Peluso, A. Explaining Different Experimental Hole Mobilities: Influence of Polymorphism on Dynamic Disorder in Pentacene. *J. Mater. Chem. C* **2019**, *7*, 9665–9670.

(50) Peluso, A.; Caruso, T.; Landi, A.; Capobianco, A. The Dynamics of Hole Transfer in DNA. *Molecules* **2019**, *24*, 4044.

(51) Parson, W. W. Temperature Dependence of the Rate of Intramolecular Electron Transfer. *J. Phys. Chem. B* **2018**, *122*, 8824–8833.

(52) Frisch, M. J.; Trucks, G. W.; Schlegel, H. B.; *al*, E.-T. Gaussian 09 Revision D.01. Gaussian Inc. Wallingford CT 2009.

(53) Xing, G.; Shuming, B.; Daniele, F.; Thomas, N.; Mario, B.; Walter, T. Evaluation of Spin-Orbit Couplings with Linear-Response Time-Dependent Density Functional Methods. *J. Chem. Theory Comput.* **2017**, *13*, 515–524.

(54) Borrelli, R.; Peluso, A. MolFC: A program for Franck-Condon integrals calculation. Package available online at `http://www.theochem.unisa.it`.

(55) Borrelli, R.; Peluso, A. Dynamics of Radiationless Transitions in Large Molecular Systems: A Franck-Condon Based Method Accounting for Displacements and Rotations of All the Normal Coordinates. *J. Chem. Phys.* **2003**, *119*, 8437–8448.

(56) Borrelli, R.; Peluso, A. The Vibrational Progressions of the N $\leftarrow$ V Electronic Transition of Ethylene. A Test Case for the Computation of Franck-Condon Factors of Highly Flexible Photoexcited Molecules. *J. Chem. Phys.* **2006**, *125*, 194308–8.

(57) Borrelli, R.; Peluso, A. The Electron Photodetachment Spectrum of c-$C_4F_8^-$: A Test Case for the Computation of Franck-Condon Factors of Highly Flexible Molecules. *J. Chem. Phys.* **2008**, *128*, 044303–7.

(58) Peluso, A.; Borrelli, R.; Capobianco, A. Photoelectron Spectrum of Ammonia, a Test Case for the Calculation of Franck–Condon Factors in Molecules Undergoing Large Geometrical Displacements upon Photoionization. *J. Phys. Chem. A* **2009**, *113*, 14831–14837.

(59) Capobianco, A.; Borrelli, R.; Noce, C.; Peluso, A. Franck-Condon Factors in Curvilinear Coordinates: The Photoelectron Spectrum of Ammonia. *Theor. Chem. Acc.* **2012**, *131*, 1181.

(60) Borrelli, R.; Capobianco, A.; Peluso, A. Franck-Condon Factors: Computational Approaches and Recent Developments. *Can. J. Chem.* **2013**, *91*, 495–504.